Journal of Alloys and Compounds 607 (2014) 50–53

Contents lists available at ScienceDirect

Journal of Alloys and Compounds

journal homepage: www.elsevier.com/locate/jalcom

# Improved anatase phase stability in small diameter $TiO_2$ nanotube arrays for high performance dye-sensitized solar cells

Xiaolin Liu [a,b], Jia Lin [a,b], Yuen Hong Tsang [b], Xianfeng Chen [a,*], Peter Hing [c], Haitao Huang [b,*]

[a] The State Key Laboratory of Advanced Optical Communication Systems and Networks, Department of Physics, Shanghai Jiao Tong University, 800 Dongchuan Road, Shanghai 200240, China
[b] Department of Applied Physics and Materials Research Center, The Hong Kong Polytechnic University, Hung Hom, Kowloon, Hong Kong
[c] Energy Group, Faculty of Science, University Brunei Darussalam (UBD), Brunei Darussalam

ARTICLE INFO

*Article history:*
Received 2 March 2014
Received in revised form 11 April 2014
Accepted 11 April 2014
Available online 20 April 2014

*Keywords:*
$TiO_2$ nanotubes
Dye-sensitized solar cells
Small diameter nanotube
Phase transitions
Electron recombination

ABSTRACT

Anatase is the preferred phase of $TiO_2$ in dye-sensitized solar cells (DSSCs) because of its lower charge recombination than other phases. However, for small diameter nanotubes before detached from the Ti foil, rutile rather than anatase appears upon a pre-treatment annealing at 400 °C or above. Here we have fabricated highly ordered free-standing small diameter (50 nm) $TiO_2$ nanotube membranes which were pre-treated at 300 °C to maintain pure anatase phase. The free-standing nanotube membranes were used to fabricate the photoanodes and were further calcined at 500 °C to achieve full crystallization of the nanotubes. It was shown that the electron lifetime is much longer in the 300 °C-pre-treated nanotubes than those pre-treated at 400 or 500 °C, leading to a significantly improved power conversion efficiency of 4.59% (enhanced by ~50%).



## 1. Introduction

$TiO_2$ nanotube arrays have received considerable attention for its good oriented charge-transport property, excellent chemical stability, and environment-friendly feature for applications in dye-sensitized solar cells (DSSCs) [1–3]. However, the efficiency of $TiO_2$ nanotube-based DSSCs is, in general, substantially lower due to the much lower surface area of nanotubes than nanoparticles. Therefore, $TiO_2$ nanotubes with large surface area have been the pursuit of a large amount of studies, among which the minimization of the nanotube diameter has become one of the important methods to enlarge the aspect ratio. A lot of attempts have been carried out to fabricate small diameters tubes [4,5] and our previous results showed that improved efficiency can be obtained by using small tubes at an anodization voltage of 20 V [6].

The specific crystal structure strongly influences the electronic properties of $TiO_2$, and the anatase phase is preferred in DSSCs because of its lower charge recombination resulting from steeper band bending [7,8]. Generally, crystallization by thermal annealing is an effective way to obtain the anatase phase. However, previous work showed a tube diameter dependent phase stabilization where rutile rather than anatase occurs upon annealing at the typical annealing temperatures for small tubes [9]. Liu et al. applied small diameter (15 nm) $TiO_2$ nanotubes to DSSCs and obtained an efficiency of only 1.59%, due to the appearance of rutile phase when the nanotubes were annealed at 450 °C [10].

Considering that the interface between rutile and anatase crystallites creates charge trapping sites with high electron recombination reactivity [8,11], in this work, we used low temperature pre-treatment (300 °C) to achieve small diameter tubes in pure anatase phase. The crystallized free-standing $TiO_2$ nanotube membranes were utilized as the photoanodes in DSSCs, showing less recombination losses and the power conversion efficiency $\eta$ reached 4.59%, showing 50% improvement as compared with the samples annealed at 500 °C.

### 2. Experimental section

Highly ordered $TiO_2$ nanotube arrays (TNAs) with small diameter were fabricated according to the reported method [12]. TNAs were synthesized through potentiostatic anodization in a conventional two-electrode electrochemical cell. Ti foil (0.125 mm in thickness, Strem Chemicals, Newburyport, MA, USA) as the working electrode was first processed under 60 V for 0.5 h in an electrolyte with a nominal composition of ethylene glycol, 0.5 wt% ammonium fluoride ($NH_4F$), and 3 vol% deionized water. The resulting oxide film was annealed at 400 °C for 2 h and was then subjected to a second anodization at 10 V for 48 h to obtain small diameter nanotubes. The film formed during the first anodization was automatically peeled off during the second anodization process. Throughout the anodization, the electrolyte was stirred by a magnetic stirrer. The as-anodized oxide films (with small

* Corresponding authors. Tel.: +86 21 54743252; fax: +86 21 54747249 (X. Chen).
*E-mail addresses:* xfchen@sjtu.edu.cn (X. Chen), aphhuang@polyu.edu.hk (H. Huang).

http://dx.doi.org/10.1016/j.jallcom.2014.04.083
0925-8388/

tubes) obtained during the second anodization were subjected to an intense ultrasonication for 30 s, followed by a pre-treatment at 300, 400 and 500 °C, respectively, for 2 h in air with a heating and/or cooling rate of 3 °C $min^{-1}$.

The synthesized small tubes were peeled off completely during a third anodization under 60 V at 30 °C for 1 h, using a method reported in [13]. After that, the free-standing membranes were exploited to fabricate front-side illuminated DSSCs. Briefly, they were attached to fluorine doped tin oxide (FTO) glasses with a thin layer (thickness ~1.5 μm) of doctor-blade coated anatase $TiO_2$ nanoparticles (average size ~20 nm, from Wuhan Geao Instruments Science and Technology Co. Ltd., China). Next, the samples were calcined again at 500 °C for 2 h to fully crystallize the TNAs since some samples were annealed at a lower temperature before detaching, and also to ensure good electrical connection between TNA membranes and FTO substrates. The as-formed photoanodes were immersed in a 1:1 (*v*/*v*) acetonitrile and tert-butylalcohol solution containing $3 \times 10^{-4}$ M N719 dye for 48 h. A 25 μm-thick hot-melt spacer separated the sensitized electrode and the counter electrode which was prepared by thermal decomposition of $H_2PtCl_6$ isopropanol solution on FTO glass at 380 °C for 30 min. The interspace was filled with a liquid electrolyte of DMPII/LiI/I2/TBP/GuSCN in 3-methoxypropionitrile.

Morphological and structural variations of the TNAs were observed by field-emission scanning electron microscope (FESEM, FEI Sirion 200) and a transmission electron microscope (TEM, JEOL JEM-2100F). X-ray diffraction (XRD, Rigaku 9KW SmartLab, Japan) analysis was performed for crystalline phase identification. The *J*–*V* characteristics were measured by a sourcemeter (Model 2420, Keithley, USA) under AM 1.5G illumination (100 mW $cm^{-2}$) which was provided by a 300 W solar simulator (Model 91160, Newport-Oriel Instruments, USA). Electrochemical impedance spectroscopy (EIS) was performed in the dark at various bias voltages with the CHI 660C electrochemical workstation (CH Instruments, USA). The amplitude of the alternative signal was 10 mV and the frequency ranged from $10^{-1}$ to $10^5$ Hz.

## 3. Result and discussion

FESEM images of small diameter TNAs are shown in Fig. 1a–c. It is well known that the nanotube diameter decreases with decreasing anodization voltage [14]. In the present work, an anodization voltage of 10 V was used (in the second anodization step) to limit the diameter of $TiO_2$ nanotubes to 50 nm, as seen from Fig. 1a–c. The TEM image in Fig. 2 also shows the formation of small diameter nanotubes.

For comparison, large diameter TNAs (of the same thickness, but with a lager diameter of about 120 nm, Fig. 1d), which were anodized at 60 V, were also fabricated. Fig. 3a and b shows XRD patterns for different diameter TNAs on the Ti foil after annealing in air at different temperatures. For small diameter TNAs (Fig. 3a), no rutile phase can be found when annealed at 300 °C, while a phase transition from anatase to rutile can be observed when annealed at 400 and 500 °C. For large diameter TNAs (Fig. 3b), this phase transition occurs at 500 °C. The percentage of the rutile phase can be estimated by the equation, $\text{Rutile}\% = A_{\text{rutile}}/(0.884A_{\text{anatase}} + A_{\text{rutile}})$, where $A_{\text{anatase}}$ and $A_{\text{rutile}}$ refer to the integrated intensities of the strongest diffraction peak of the anatase and rutile phases, respectively [15]. The results (Fig. 3c) suggested that the rutile content at 300 °C was 0 and it increased to 9.1% and 15.9% after calcination at 400 and 500 °C, respectively. This is due to the "substrate effect", that is, when the metallic Ti substrate was oxidized, a thin compact rutile layer was directly formed at the interface, which initiate the observed phase transition in TNAs [8,16,17]. As estimated from the Scherrer's equation [18], the average crystallite size of the small diameter NTAs (~22 nm) is smaller than the large ones (~30 nm). The small crystallites are unstable and inclined to coalesce together [19], resulting in a much more severe "substrate effect" observed in small diameter TNAs. Indeed, for large diameter TNAs which

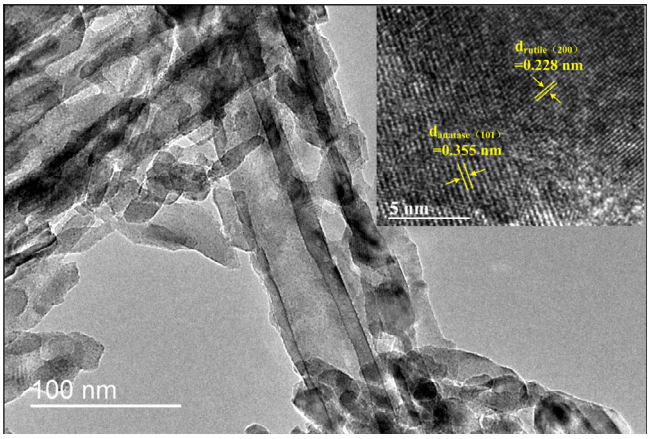


**Fig. 2.** TEM image of the small diameter nanotubes (pre-annealed at 500 °C). Inset: HRTEM image, showing the coexistence of rutile and anatase.

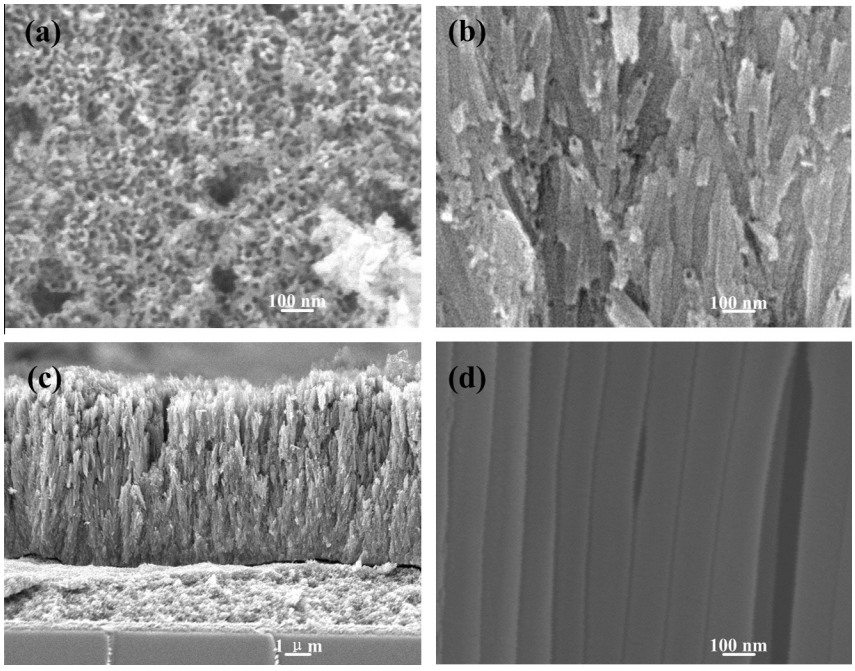


**Fig. 1.** FESEM images of (a) the top and the cross-sections of (b and c) small and (d) large diameter TNAs.

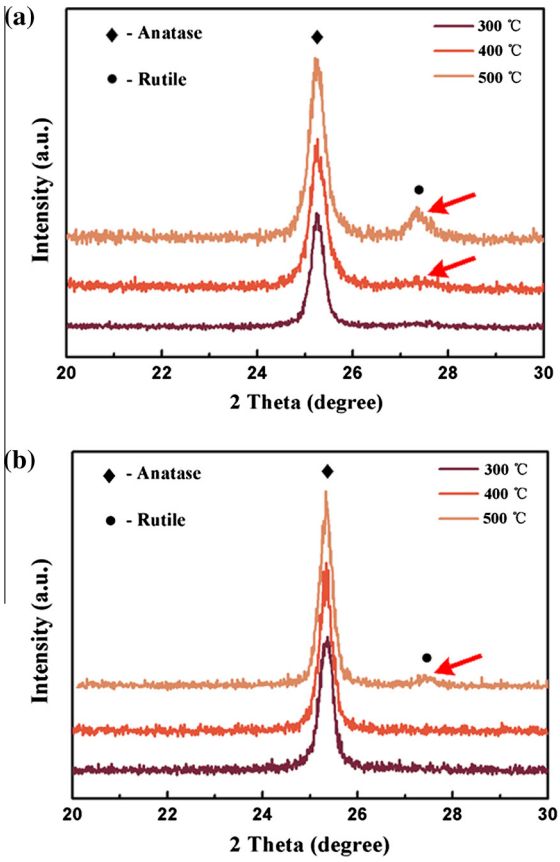


(c)

| Rutile fraction | | |
|---|---|---|
| Samples | 10 V | 60 V |
| 300 ℃ | 0 | 0 |
| 400 ℃ | 9.1% | 0 |
| 500 ℃ | 15.9% | 8.6% |

**Fig. 3.** XRD patterns of the top of (a) small diameter, (b) large diameter TNAs before detached from Ti foils. (c) Summary of the phase composition of the TNAs membranes.

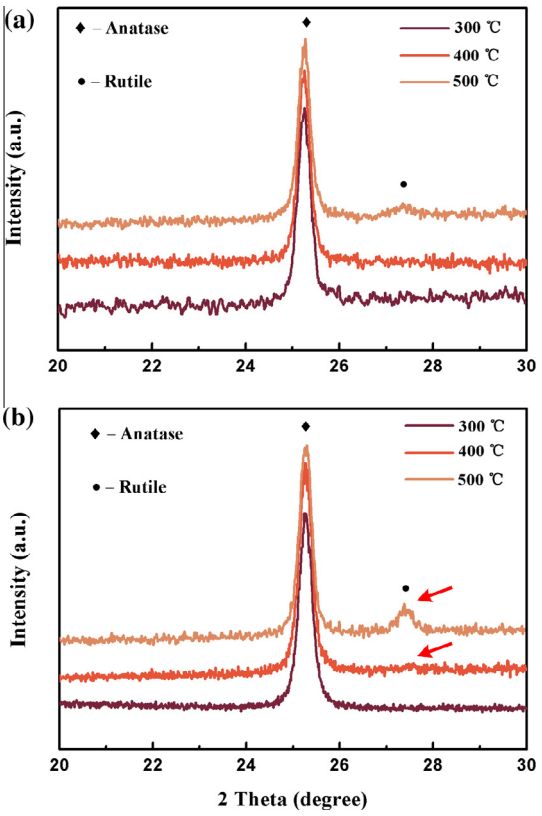


**Fig. 4.** The XRD patterns of (a) the top and (b) the bottom of the free-standing small nanotube membranes.

were anodized at 60 V, the anatase to rutile phase transition temperature is retarded to 500 °C (Fig. 3c).

Fig. 4 shows the XRD patterns of the top and bottom of the 500 °C-annealed free-standing small diameter TNA membranes that were pre-treated at different temperatures (300, 400 and 500 °C). It can be seen that this pre-treatment does affect the phase even though the final annealing temperature is the same (500 °C) for all the samples. No rutile phase can be detected in TNAs pre-treated at 300 °C. Due to the absence of the influence of the "substrate" for the free-standing membrane, the TNAs can maintain in anatase phase up to 500 °C [15]. While for TNAs pre-treated at 400 and 500 °C, tiny amount of rutile phase has already been developed at the bottom of nanotubes which acts as nucleation sites for the growth of rutile phase in the final annealing at 500 °C. The HRTEM image of the small diameter nanotubes pre-treated at 500 °C (Fig. 2) shows the coexistence of the anatase (*d*-spacing of 0.355 nm, (101) plane) and the rutile (*d*-spacing of 0.228 nm, (200) plane) phases. Also, as seen from Fig. 4, the rutile peak was more pronounced at the bottom than at the top of the nanotube membrane, indicating the "substrate effect" on the formation of rutile phase. It should be noted that, during the pre-treatment annealing, the rutile crystals predominantly exist at the nanotube-Ti metal interface region, which results in less rutile being detected from the bottom of the free-standing TNAs when they were peeled off from the Ti substrate (Fig. 4 as compared to Fig. 3a).

These small diameter TNA membranes pre-treated at different annealing temperatures were exploited as photoanodes of DSSCs. The photocurrent density *vs.* voltage (*J*–*V*) and the characteristic photovoltaic parameters were shown in Fig. 5. It can be seen that the short-circuit current density ($J_{SC}$) decreases with increasing pre-treatment annealing temperatures due to the more trap densities and hence more electron recombination associated with the rutile phase in TNAs pre-treated at higher temperatures [19]. The higher trap densities and larger electron recombination probability also result in decreased open-circuit voltages ($V_{OC}$) in samples with more rutile phases, i.e., pre-treated at higher temperatures. Consequently, due to the maintenance of pure anatase phase in the sample pre-treated at a low temperature (300 °C), a significant increase in power conversion efficiency ($\eta$) of ~50% can be achieved, as compared with the sample pre-treated at 500 °C ($\eta$ increased from 3.10% to 4.59%). The $\eta$ of DSSC equipped with large diameter TNAs is also compared in Fig. 5.

To analyze the electron recombination behaviors in DSSCs based on the small diameter TNAs, electrical impedance spectroscopy (EIS) was performed in dark under various biased voltages. The electron lifetime ($\tau_n$) was calculated from the Bode phase plots by $\tau_n = 1/(2\pi f_{peak})$, where $f_{peak}$ is the characteristic peak frequency in the mid frequency (1–100 Hz) region [20]. As shown in Fig. 5b, the lifetime for TNAs pre-treated at low annealing temperature (300 °C) is the highest, due to reduced surface traps and lower

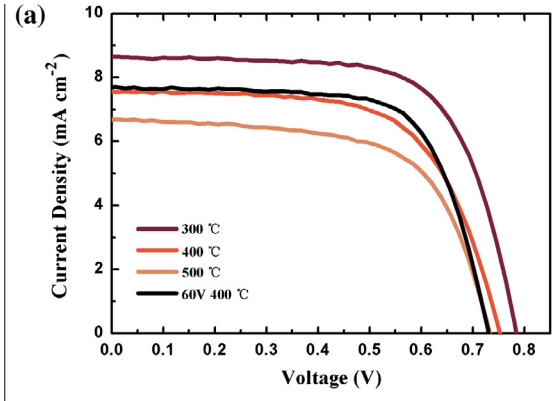


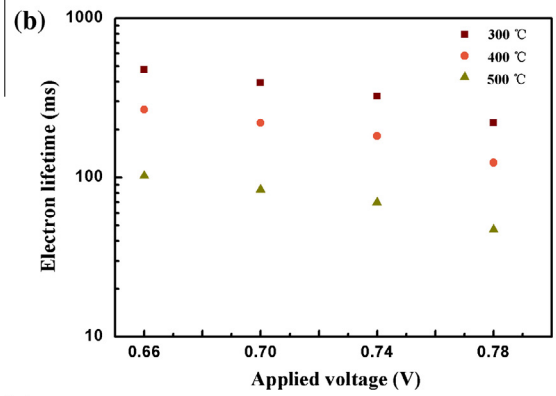


(c)

| Annealing temperature | $J$sc (mA cm$^{-2}$) | $V$oc(V) | $FF$ | Relative Dye loading | $\eta$ (%) |
|---|---|---|---|---|---|
| 300 ℃ | 8.65 | 0.79 | 67.7 | 0.351 | 4.59 |
| 400 ℃ | 7.56 | 0.75 | 64.1 | 0.357 | 3.64 |
| 500 ℃ | 6.68 | 0.73 | 63.4 | 0.356 | 3.10 |
| 60V 400 ℃ | 7.69 | 0.73 | 69.4 | 0.224 | 3.90 |

**Fig. 5.** (a) $J$–$V$ characteristics of DSSCs based on different diameter TNAs pre-treated at different temperatures. (b) Electron lifetime of DSSCs as a function of bias voltages. (c) The photovoltaic parameters of DSSCs based on different diameter TNAs.

probability of electron recombination in pure anatase phase. The electron lifetime in TNAs pre-treated at 300 °C is about 4 times the value in TNAs pre-treated at 500 °C, which is the dominant factor for the significantly increased photocurrent observed (Fig. 5a).

## 4. Conclusion

Overall, by lowering the pre-treatment annealing temperature, we have successfully peeled off the small diameter TNAs from the Ti substrate and applied them as the photoanode in DSSCs. Pure anatase phase was maintained (for samples pre-treated at 300 °C) in the subsequent annealing at 500 °C due to the removal of "substrate effect". It is found that the electron lifetime in TNAs pre-treated at 300 °C is about four times the value in the sample pre-treated at a higher temperature of 500 °C, mainly due to the pure anatase phase with reduced electron trap density as compared with rutile phase. The resultant conversion efficiency of the small diameter TNAs-based DSSCs with pure anatase phase is significantly enhanced by ~50%, as compared with the TNAs pre-treated at a higher temperature of 500 °C. Pure anatase phase with good crystallinity is of crucial importance to the improvement of photovoltaic performance of DSSCs.

## Acknowledgements

The work was supported by grants received from the Research Grants Council of the Hong Kong Special Administrative Region (Project Nos. PolyU5159/13E and PolyU5163/12E) and the Hong Kong Polytechnic University (Project No. G-YL06). The work was also supported by the National Natural Science Foundation of China (Grant No. 61125503) and the Foundation for Development of Science and Technology of Shanghai (Grant No. 11XD1402600).

## References

[1] C.T. Yip, H. Huang, L. Zhou, K. Xie, Y. Wang, T. Feng, J. Li, W.Y. Tam, Adv. Mater. 23 (2011) 5624.
[2] M. Guo, K. Xie, J. Lin, Z. Yong, C.T. Yip, L. Zhou, Y. Wang, H. Huang, Energy Environ. Sci. 5 (2012) 9881.
[3] J.M. Macak, H. Tsuchiya, A. Ghicov, P. Schmuki, Electrochem. Commun. 7 (2005) 1133.
[4] S. Liang, J. He, Z. Sun, Q. Liu, Y. Jiang, H. Cheng, B. He, Z. Xie, S. Wei, J. Phys. Chem. C 116 (2012) 9049.
[5] A. Ghicov, S.P. Albu, R. Hahn, D. Kim, T. Stergiopoulos, J. Kunze, C.-A. Schiller, P. Falaras, P. Schumki, Chem. Asian J. 4 (2009) 520.
[6] X. Liu, J. Lin, X. Chen, RSC Adv. 3 (2013) 4885.
[7] T. Sumita, T. Yamaki, S. Yamamoto, A. Miyashita, Appl. Surf. Sci. 200 (2002) 21.
[8] K.L. Schultev, P.A. DeSario, K.A. Gray, Appl. Catal. B 97 (2010) 354.
[9] S. Bauer, A. Pittrof, H. Tsuchiya, P. Schmuki, Electrochem. Commun. 13 (2011) 538.
[10] N. Liu, K. Lee, P. Schmuki, Electrochem. Commun. 15 (2012) 1.
[11] D.C. Hurum, K.A. Gray, J. Phys. Chem. B 109 (2005) 977.
[12] G. Liu, N. Hoivik, K. Wang, Electrochem. Commun. 28 (2013) 107–110.
[13] J. Lin, J. Chen, X. Chen, Electrochem. Commun. 12 (2010) 1062.
[14] G. Zhang, H. Huang, Y. Zhang, H.L.W. Chan, L. Zhou, Electrochem. Commun. 9 (2007) 2854.
[15] A.A. Gribb, J.F. Banfield, Am. Mineral. 82 (1997) 717.
[16] K. Zhu, N.R. Neale, A.F. Halverson, J.Y. Kim, A.J. Frank, J. Phys. Chem. C 114 (2010) 13433.
[17] Y. Yang, X.H. Wang, L.T. Li, J. Am. Ceram. Soc. 91 (2008) 632.
[18] H.P. Klug, L.E. Alexander, John Wiley & Sons, New York, 1962, p. 491.
[19] J. Lin, M. Guo, G. Yip, W. Lu, G. Zhang, X. Liu, L. Zhou, X. Chen, H. Huang, Adv. Funct. Mater. 23 (2013) 5952.
[20] R. Kern, R. Sastrawan, J. Ferber, R. Stangl, J. Luther, Electrochim. Acta 47 (2002) 4213.